

## Supporting information

### Degradation induced Lattice Anchoring Self-passivation in $\text{CsPbI}_{3-x}\text{Br}_x$

Jingwei Xiu,<sup>1,2</sup> Bo Dong<sup>1</sup>, Elizabeth Driscoll<sup>1</sup>, Xiyuan Feng<sup>2</sup>, Abubakar Muhammad<sup>1</sup>,  
Shaoqing Chen<sup>3</sup>, Zheng Du<sup>2</sup>, Yudong Zhu<sup>2</sup>, Zheng Zhang<sup>2</sup>, Zhaoheng Tang<sup>2</sup>, Zhubing He<sup>\*,2</sup>,  
Peter Raymond Slater<sup>\*,1</sup>

#### Method

##### *Characterization:*

*Powder X-ray diffraction (PXRD) measurements were performed on a Bruker D8 Diffractometer with Cu K $\alpha$  radiation in ambient environment. Scanning Electron Microscopy (SEM) images were collected using a TESCAN MIRA3 instrument, operating at an accelerating voltage of 10 kV. X-ray Photoelectron Spectroscopy (XPS) measurements were performed on an ESCALAB 250Xi Thermo Fisher instrument (by using Al K $\alpha$  X-ray source) under high vacuum ( $10^{-9}$  mbar). The XPS spectra were calibrated by the binding energy of C 1s. High-resolution transmission electron microscopy (TEM) images were recorded on a FEI Tecnai F30 with acceleration voltage of 80 kV. A FEI Talos Transmission Electron Microscope (TEM) with Super-X EDX (Energy Dispersive X-Ray Analysis) was employed to acquire the STEM-EDX data with high-angle annular dark field (STEM-HAADF) mode. Photo-luminescence (PL) measurements were carried out using a spectrofluorometer (FS5, Edinburgh instruments), with a 405 nm pulsed laser used as excitation sources. Fourier Transform Infrared Spectroscopy (FTIR) was performed using an Agilent Technologies Cary 630 FTIR spectrometer.*

### ***Structure refinements***

*Structure refinements of CsPbI<sub>3</sub> and CsPbI<sub>2</sub>Br were carried out using XRD data. CsPbI<sub>3</sub> with Pmna space group was chosen as a starting model, and  $U_{iso}$  of each atom was set to a default value, 0.01 Å<sup>2</sup>. The scale factor, background (12 terms of shifted Chebyshev function) and lattice parameters were refined. Then, peak profile coefficient and preferred orientation factor were refined and fixed after convergency. The atomic coordinates of Pb1, Cs1, I1 and I2 were refined followed by  $U_{isos}$  of Pb1, Cs1, I1 and I2, which were refined together in the last step. Structure information for CsPbI<sub>3</sub> is shown in SI table 1a.*

*A similar structure refinement for CsPbI<sub>2</sub>Br was conducted. A constraint of the same atomic coordinates and  $U_{isos}$  with overall full site occupancy ( $I2 + Br2 = 1$ ) was used initially. The refinement gave occupancies of 0.52(2) for I2 and 0.48(2) for Br2 which is consistent with expected composition within 1 esd. Final refined parameters of CsPbI<sub>2</sub>Br are shown in SI table 1b.*

## Figures

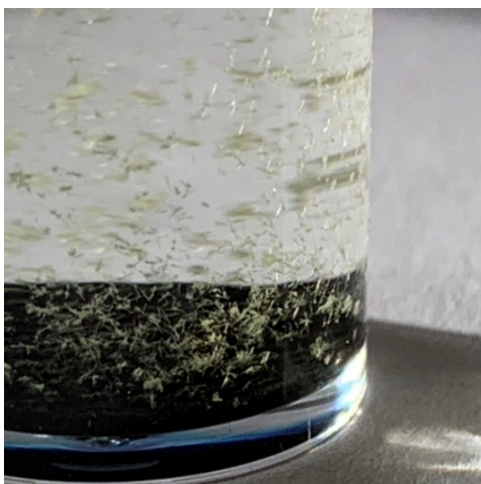


Fig S1 Photograph of yellow needle-like  $\delta$ -CsPbI<sub>3</sub> crystals slowly growing on the wall of the sample bottle, with rapidly formed  $\gamma$ -CsPbI<sub>3</sub> already settled down to the bottom.

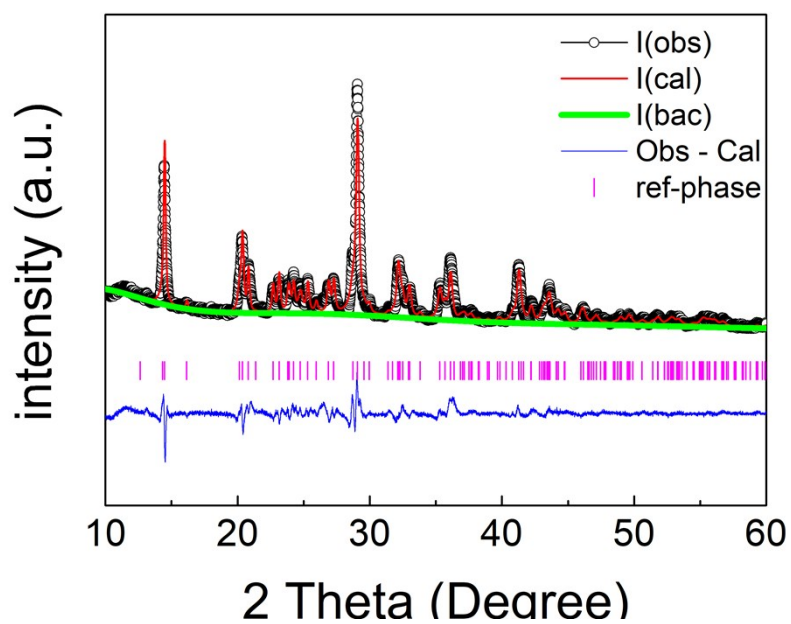


Fig S2 Observed, calculated and difference profiles for CsPbI<sub>3</sub>@PbI(OH) from Rietveld refinement of the structure using powder XRD data.

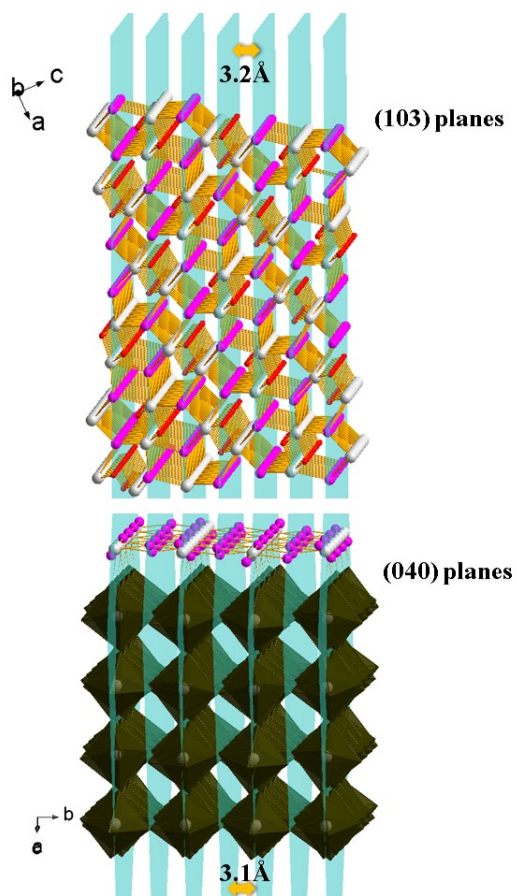


Fig S3 Atom distributions in (103) planes of  $\text{PbI}(\text{OH})$  and (040) planes of perovskite. White: lead, Purple: Iodide, Red: Oxygen.

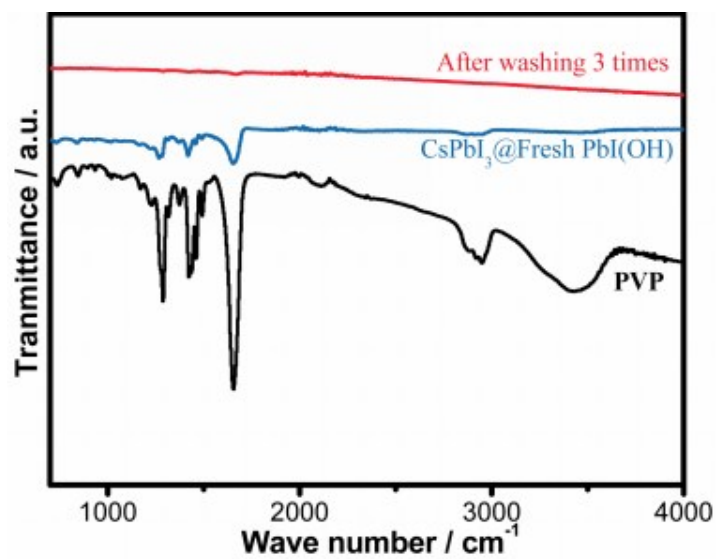


Fig S4 Fourier Transform Infrared Spectrum (FTIR) spectrum of PVP and  $\gamma\text{-CsPbI}_3\text{@PbI}(\text{OH})$  before and after washing with isopropanol, showing removal of the PVP.

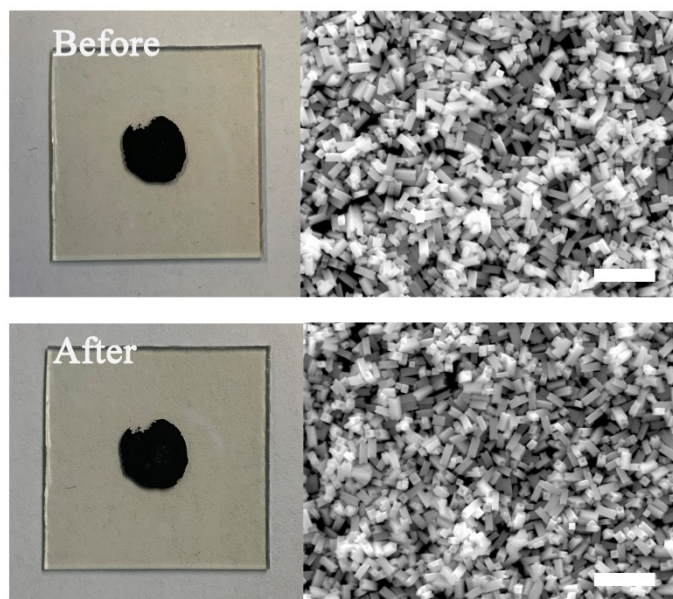


Fig S5 Digital photos and SEM images of  $\text{CsPbI}_3@\text{PbI}(\text{OH})$  before and after stability test (heating at  $175^\circ\text{C}$  in air for 12h) .

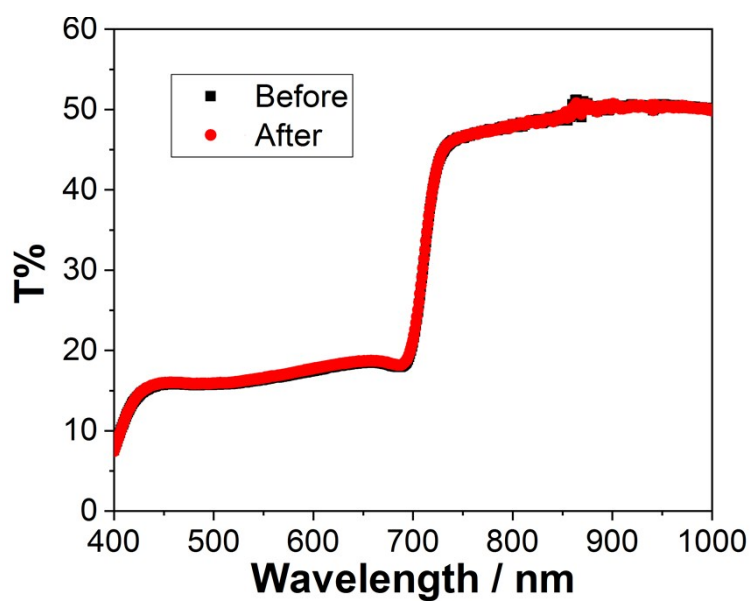


Fig S6 UV-Vis transmittance analysis of  $\text{CsPbI}_3@\text{PbI}(\text{OH})$  film before and after stability test. The film was fabricated by spin-coating  $\text{CsPbI}_3@\text{PbI}(\text{OH})$  colloids on ITO glass.



Fig S7 Demonstration of scale-up preparation of  $\gamma$ -CsPbI<sub>3</sub>@PbI(OH).

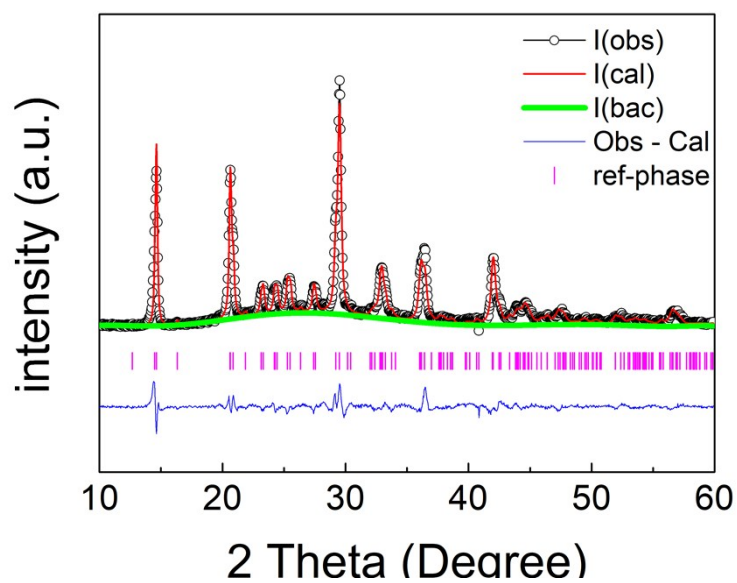


Fig S8 Observed, calculated and difference profiles for CsPbI<sub>2</sub>Br@PbI(OH) from Rietveld refinement of the structure using powder XRD data.

Table 1a Refined structural parameters for CsPbI<sub>3</sub>

| Atom | <i>x</i>  | <i>y</i>  | <i>z</i>  | Mult. | Occupancy | <i>u</i> <sub>iso</sub> ×100 (Å <sup>2</sup> ) |
|------|-----------|-----------|-----------|-------|-----------|--|
| Pb1  | 0         | 0         | 0         | 4     | 1         | 1.7(1)   |
| Cs1  | 0.4459(5) | 0.25      | 0.0153(6) | 4     | 1         | 3.6(2)   |
| I1   | 0.5091(6) | 0.25      | 0.5645(5) | 8     | 1         | 2.2(2)   |
| I2   | 0.1959(3) | 0.0273(3) | 0.3103(3) | 4     | 1         | 0.9(1)   |

---

*a* = 8.867(1)Å, *b* = 12.472(1)Å, *c* = 8.579(1)Å, *V* = 948.80(7)Å<sup>3</sup>

GOF = 2.17, wR = 6.18%

---

Table 1b Refined structural parameters for CsPbI<sub>2</sub>Br

| Atom | <i>x</i>   | <i>y</i>   | <i>z</i>   | Mult. | Occupancy | <i>u</i> <sub>iso</sub> ×100 (Å <sup>2</sup> ) |
|------|------------|------------|------------|-------|-----------|--|
| Pb1  | 0          | 0          | 0          | 4     | 1         | 1  |
| Cs1  | 0.4556(11) | 0.25       | 0.0088(17) | 4     | 1         | 1  |
| I1   | 0.5085(15) | 0.25       | 0.5575(14) | 4     | 1         | 1  |
| I2   | 0.1988(12) | 0.0247(11) | 0.3012(12) | 8     | 0.52(2)   | 1  |
| Br2  | 0.1988(12) | 0.0247(11) | 0.3012(12) | 8     | 0.48(2)   | 1  |

---

*a* = 8.598(1)Å, *b* = 12.224(2)Å, *c* = 8.496(1)Å, *V* = 892.25(15)Å<sup>3</sup>

GOF = 2.53, wR = 8.11%

---

Table 1 a, Refined structural parameters for CsPbI<sub>3</sub>@PbI(OH). b, Refined structural parameters for CsPbI<sub>2</sub>Br@PbI(OH).